

IL-34 and M-CSF form a novel heteromeric cytokine and regulate the M-CSF receptor activation and localization

Aude Segaliny, Régis Brion, Bénédicte Brulin, Mike Maillasson, Céline Charrier, Stéphane Téletchéa, Dominique Heymann

▶ **To cite this version:**

Aude Segaliny, Régis Brion, Bénédicte Brulin, Mike Maillasson, Céline Charrier, et al.. IL-34 and M-CSF form a novel heteromeric cytokine and regulate the M-CSF receptor activation and localization: IL-34/M-CSF: a new heteromeric cytokine. Cytokine, 2015, 76 (2), pp.170 - 181. 10.1016/j.cyto.2015.05.029 . inserm-01644778

HAL Id: inserm-01644778

https://inserm.hal.science/inserm-01644778

Submitted on 22 Nov 2017

HAL is a multi-disciplinary open access archive for the deposit and dissemination of scientific research documents, whether they are published or not. The documents may come from teaching and research institutions in France or abroad, or from public or private research centers.

L'archive ouverte pluridisciplinaire **HAL**, est destinée au dépôt et à la diffusion de documents scientifiques de niveau recherche, publiés ou non, émanant des établissements d'enseignement et de recherche français ou étrangers, des laboratoires publics ou privés.

IL-34 and M-CSF form a novel heteromeric cytokine and regulate the M-CSF receptor activation and localization

SÉGALINY Aude I. [1,2], BRION Régis[1,2,3], BRULIN Bénédicte[1,2], MAILLASSON Mike[4], CHARRIER Céline[1,2], TELETCHEA Stéphane[5], HEYMANN Dominique[1,2,3]

[1]INSERM, UMR 957, Equipe Ligue 2012, Nantes F-44035, France

[2]Université de Nantes, Laboratoire de Physiopathologie de la Résorption Osseuse et Thérapie des Tumeurs Osseuses Primitives, France

[3] Centre hospitalier universitaire de Nantes, France

[4]INSERM, U892; CNRS, U6299, Centre de Recherche en Cancérologie Nantes-Angers, Plateforme IMPACT, SFR Bonamy, Université de Nantes, France.

[5] FIP, UMR CNRS 6286, Faculté des Sciences et Techniques, Université de Nantes, France.

Running title: IL-34/M-CSF: a new heteromeric cytokine

***Corresponding authors:**
Prof. Dominique Heymann
INSERM UMR 957, Faculty of Medicine,
1 rue Gaston Veil, 44035 Nantes cedex, France
Phone: 33 (0) 272 641 132; Fax: 33 (0) 240 412 860
E-mail: dominique.heymann@univ-nantes.fr

ABSTRACT

Interleukin-34 (IL-34) is a newly-discovered homodimeric cytokine that regulates, like Macrophage Colony-Stimulating Factor (M-CSF), the differentiation of the myeloid lineage through M-CSF receptor (M-CSFR) signaling pathways. To date, both cytokines have been considered as competitive cytokines with regard to the M-CSFR. The aim of the present work was to study the functional relationships of these cytokines on cells expressing the M-CSFR. We demonstrate that simultaneous addition of M-CSF and IL-34 led to a specific activation pattern on the M-CSFR, with higher phosphorylation of the tyrosine residues at low concentrations. Similarly, both cytokines showed an additive effect on cellular proliferation or viability. In addition, BIAcore experiments demonstrated that M-CSF binds to IL-34, and molecular docking studies predicted the formation of a heteromeric M-CSF/IL-34 cytokine. A proximity ligation assay confirmed this interaction between the cytokines. Finally, co-expression of the M-CSFR and its ligands differentially regulated M-CSFR trafficking into the cell. This study establishes a new foundation for the understanding of the functional relationship between IL-34 and M-CSF, and gives a new vision for the development of therapeutic approaches targeting the IL-34/M-CSF/M-CSFR axis.

Keywords: Interleukin-34; Macrophage-Colony Stimulating Factor; Heteromeric cytokine; cFMS trafficking; molecular modeling

1. INTRODUCTION

Interleukin-34 (IL-34), discovered six years ago, acts as a "twin" cytokine for Macrophage Colony-Stimulating Factor (M-CSF), exerting its roles through a common receptor, the M-CSF receptor (M-CSFR) [1]. M-CSF and IL-34 redundancy is illustrated by studies of M-CSFR knockout mice that exhibit a more severe phenotype [2] than *op/op* mice which only have an inactivation of the M-CSF gene [3,4] . In addition, expression of the IL-34 gene under the M-CSF promoter rescues the phenotype of the *op/op* mice [5]. IL-34 supports the proliferation and survival of the myeloid lineage, but also drives monocyte differentiation into macrophages [6]. More specifically, macrophage polarization induced by M-CSF and IL-34 is similar, as both cytokines lead to immunosuppressive macrophages M2 [7]. In addition, IL-34 promotes osteoclastic differentiation with almost the same efficiency as M-CSF [8]. However, IL-34 may also display singular functions, as supported by a different expression pattern of M-CSF and IL-34 during brain development, thus suggesting complementary activities for these "twins" [9]. The differential expression of M-CSF and IL-34, with respect to M-CSFR expression, may be related to their own specific activities. The recent establishment of IL-34 knockout mice showed a specific role of the cytokine in the development of Langerhans cells and microglia and is consequently in favor of specific activities for both cytokines [10]. Consistent with these findings, Chihara *et al*. observed notable differences in human immunodeficiency virus (HIV) replication and activation of the MAPK pathway in macrophages differentiated with M-CSF or IL-34 [11].

Compared to M-CSF, IL-34 is reported to have better affinity for the M-CSFR, which displays intrinsic tyrosine kinase activity and activates intracellular signaling cascades after ligand binding [12]. Recently, structural studies of M-CSFR activation following M-CSF or IL-34 binding have shed light on their overlapping and independent roles. IL-34 and M-CSF remain surprising glycoproteins as they do not share any homology in their primary protein sequences, despite similar folding as seen by the tridimensional structure of their homodimers. Both cytokines are effectively produced as homodimeric glycoproteins, with a helical structure. M-CSF's tertiary structure is composed of two small β-sheets and four α-helices paired with intra-chain disulfide bonds [13]. IL-34 shares M-CSF's four-helical bundle core fold, but the β-strands are shorter and partially substituted by three other short helix. Hence, IL-34 belongs to the short-chain helical cytokine family, despite the singular localization of its intra-molecular disulfide bonds [14,15]. After translation and N-glycosylation in the endoplasmic reticulum, M-CSF proteins are rapidly dimerized thanks to inter-chain disulfide bonds [16]. However, the main and original characteristic of IL-34 remains its structural plasticity, associated with its small and hydrophobic dimerization interface in its non-covalent dimeric form [15]. These two related "twin" cytokines use a similar bivalent mode for binding to the M-CSFR, leading to homotypic M-CSFR/M-CSFR interactions through their D4 domain [17]. The M-CSFR belongs to the class III receptor-type tyrosine kinases, exhibiting five Ig-like extracellular domains [18]. Like M-CSF, IL-34 binds to the first three D1-D3 extracellular domains of the receptor with similar structural and mechanistic features [19]. Thus, IL-34/M-CSFR and M-CSF/M-CSFR complexes are highly similar in geometry and molecular

assembly [19]. Although murine IL-34 and M-CSFR target and cover the same areas on the M-CSFR, distinct interactions are implemented for each ligand [12]. Hydrogen-bonding interactions between M-CSF and M-CSFR are replaced by hydrophobic interactions in the IL-34/M-CSFR complex. Consequently, these differences in the interface composition result in a rearrangement of the receptor domains in the IL-34/M-CSFR complex, explaining the higher affinity of IL-34 for the M-CSFR compared to M-CSF [15].

The present study focuses on the interactions between these non-homologous ligands, and on their functional consequences on M-CSFR-expressing cells. Here, we demonstrate that simultaneous addition of M-CSF and IL-34 led to a specific activation pattern on the M-CSFR, with higher phosphorylation of the tyrosine residues at low concentrations. Similarly, both cytokines showed an additive effect on cellular proliferation or viability. The absence of the previously reported competitive effects between the “twins” can be explained by the formation of a heteromeric M-CSF/IL-34 cytokine predicted by molecular docking studies. This interaction between M-CSF and IL-34 was confirmed by surface plasmon resonance and proximity ligation assays. In addition, co-expression of the M-CSFR and its ligands differentially regulates the receptor’s glycosylation state and localization in the cell. This is the first report demonstrating the direct interaction between IL-34 and M-CSF and their ability to form a new heteromeric cytokine that may play a part in the tissue homeostasis and development.

2. MATERIAL AND METHODS

2.1. Reagents

Recombinant human glycosylated interleukin-34 (IL-34), Macrophage Colony-Stimulating Factor (M-CSF), Macrophage Colony-Stimulating Factor Receptor (M-CSFR) and Receptor activator of nuclear factor kappa-B ligand (RANKL) were obtained from R&D Systems (Abingdon, UK). Anti-human M-CSFR for immunofluorescence, flow cytometry and Western blot were respectively from eBiosciences (Paris, France), R&D and Cell Signaling (Ozyme, Saint Quentin Yvelines, France). Antibodies for Western blot directed against the phospho-tyrosines 708, 723 and 923 of M-CSFR, phospho-Erk1/2, and total Erk1/2 were purchased from Cell Signaling, and β-actin from Sigma-Aldrich (Saint Quentin Fallavier, France). Horseradish peroxidase-conjugated secondary antibodies were obtained from Santa-Cruz (CliniSciences, Nanterre, France). Polyclonal anti-human M-CSF antibodies were purchased from R&D Systems for blocking activities and from Life Span Biosciences (CliniSciences) for immunofluorescence. Monoclonal anti-human antibodies against IL-34 used for immunofluorescence and flow cytometry were respectively obtained from Diaclone (Besançon, France) and R&D Systems. The Alamar-Blue® cell viability assay was purchased from Life Technologies (Villebon sur Yvette, France) and the Duolink® *in situ* PLA Technology from Olink Bioscience. The Tartrate Resistance Phosphatase Acid assay (TRAP), cycloheximide, tunicamycin, Brefeldin A, Dimethyl sulfoxide (DMSO), saponin and other biochemical reagents were purchased from Sigma-Aldrich. Cell culture products were obtained from Lonza (Levallois-Perret, France). Prolong Gold antifade reagent (Molecular Probes) was ordered from Life Technologies.

Alexa fluor 488 anti-rat, alexa fluor 568 Phalloidin and DAPI (4',6-Diamidino-2-Phenylindole, Dihydrochloride) were obtained from Invitrogen (Life Technologies) and Draq 5 from Eurobio/Biostatus (Courtaboeuf, France).

2.2. Cloning of the human M-CSFR gene

The human M-CSFR gene (*c-fms,* Accession number NM_005211.3) was cloned in a pCDNA3.3 TOPO TA vector (Life Technologies) from the cDNA of $CD14^+$ cells from a healthy donor (Etablissement Français du Sang, Nantes, France). RT-PCR was carried out using the following primers: Forward CACCATGGGCCCAGGAGTTCTGCTGCT and Reverse AACTCCTCAGCAGAACTGATAGTTGTTGGGCTGCA. Denaturation, hybridation and elongation cycles were done with the MiniBiorad (Biorad, Marnes-la-Coquette, France). The M-CSFR gene was ligated in the pCDNA3.3 TOPO TA vector, then competent DH5-α Max efficiency cells (Life Technologies) were transformed. Minipreps were prepared from the colonies obtained using the Nucleospin Plasmid kit (Macherey Nagel, Duren, Germany). Plasmids containing the gene of interest were then fully sequenced to check for the presence of mutations compared to the initial sequence (SFR Bonamy, Genomic facility, University of Nantes).

2.3. Cell cultures

HEK293 (ATCC® Number: CRL-1573™), osteosarcoma MG-63 (ATCC® Number: CRL-1427™) and MNNG/HOS (ATCC® Number: CRL-1547™) cells were cultured in DMEM (Dulbecco's Modified Eagle's Medium, Lonza) supplemented with 10% fetal bovine serum (FBS; Hyclone Perbio, Bezons, France) and 2 mmol/L L-glutamine. THP-1 (ATCC®

Number: TIB-202™) were maintained in RPMI (Roswell Park Memorial Institute, Lonza) medium supplemented with 10% FBS. The TF-1 cell line (ATCC® Number: CRL-2003™) was also cultured in RPMI medium with 10% FBS, and 3 ng/mL of GM-CSF following ATCC recommendations. The modified HEK, HOS and TF-1 cell lines (Mock or M-CSFR), as well as MG-63 (clone 2A8), were respectively cultured in a selective medium with 0.5 mg/mL of G418 or 4 µg/mL of puromycin.

$CD14^+$ were obtained from peripheral blood mononuclear cells isolated by centrifugation over Ficoll gradient (Sigma) from the blood of five healthy donors (Etablissement Français du Sang, Nantes, agreement referenced NTS 2000-24, Avenant n°10). $CD14^+$ cells were magnetically labeled with CD14 microbeads and positively selected by MACS technology (Miltenyi Biotec, Bergisch Gladbach, Germany). The purity of the cells was assessed by flow cytometry (Cytomics FC500; Beckman Coulter, Villepinte, France) and was > 95%. The $CD14^+$ were cultured in α-MEM medium (Minimum Essential Medium, Lonza) supplemented with 10% FBS.

2.4. Stable and transient modified cell lines

Embryonic HEK293 cells and osteosarcoma MNNG/HOS cells were transfected as described below with the pCDNA3 empty plasmid or the pCDNA3 plasmid containing the M-CSFR gene. To obtain a polyclonal population expressing the M-CSFR, $5x10^6$ cells were then stained with phycoerythrin (PE) conjugated antibodies directed against the M-CSFR and sorted out on a FACSAria III (BD Biosciences, Le Pont de Claix Cedex, France). The cells expressing the M-CSFR were named respectively HEK M-CSFR and HOS M-CSFR.

Cells that only transfected the empty pCDNA3 vector were called HEK Mock and HOS Mock. Erythroblastic TF-1 cells were transfected using an Amaxa® Cell Line Nucleofector® Kit from Lonza and the M-CSFR-expressing cells were isolated by flow cytometry. Cells transfected with the empty pCDNA3 vector or the vector containing the M-CSFR gene were respectively named TF-1 Mock and TF-1 M-CSFR. Osteosarcoma MG-63 cells expressing human IL-34 were obtained after cationic liposome-mediated transfection with a vector pEZ-Lv105 (GeneCopoeia, Rockville, USA) containing the human IL-34 gene (Accession Number BC029804). Clones were then obtained after serial dilutions in a selective medium containing puromycin (Sigma-Aldrich).

The pEZ-Lv105 vector (GeneCopoeia, Rockville, USA) containing either the human IL-34 gene (Accession Number BC029804) or the human M-CSF gene (Accession number NM_000757) were used for transient transfections. Transfections were performed with either jetPEI® (Polyplus-transfection, Illkirch, France) or Lipofectamine 2000™ (Life Technologies) according to the manufacturers' instructions.

Several siRNA directed against the M-CSF gene were designed using Reynolds' criteria [20] and Naito's recommendations [21]. The efficiency of the siRNA designed (Eurogentec, Angers, France) was assessed after transfection at 2.5, 5, 10 and 20 nM with interferin® (PolyPLus transfection, Saint Quentin Yvelines, France) into the M-CSF-expressing HOS cells. Down-regulation of the M-CSF gene expression was measured at 24, 48 and 72 hours by RT-qPCR and various other genes were also tested to check for off-target effects. Three validated siRNAs, siM-CSF$_{621}$ (sense strand: GTA GAC CAG GAA CAG TTG A), siM-CSF$_{758}$ (sense strand: GCT TCA CCA AGG ATT ATG A) and siM-

CSF_{952} (sense strand: GCC AAG ATG TGG TGA CCA A) were then transfected into HOS M-CSFR cells. An siRNA targeting the luciferase gene (named siLucF, sense strand: CUU ACG CUG AGU ACU UCG A) was used as the negative control.

2.5. Proliferation assays

The effects of IL-34 and M-CSF on $CD14^+$ survival/proliferation were determined by measuring metabolic activity using an Alamar Blue® assay. Forty thousand cells per well were put into 96-well plates with α-MEM and 5 or 10 ng/mL of M-CSF or IL-34 (10 wells per condition for each donor). After 3 days, Alamar blue® reagent was added and the fluorescence produced was read in the linear range (excitation 530 nm/emission 600 nm). For the TF-1 M-CSFR cell line, 10^4 cells per well were put (in quadruplicate) into 48-well plates with RPMI medium, 1% FBS and 5 or 10 ng/mL of cytokines. Fresh medium was added every two days, cells were harvested after 7 days of culture and counted manually. Experiments were performed three times. A similar assay was also performed on TF-1 M-CSFR cells with 25 ng/mL of cytokines in the presence of 2 µg/mL of a M-CSF blocking antibody, where viability was measured after 7 days with an Alamar blue® assay.

2.6. Osteoclastogenesis assay

Forty-five thousand $CD14^+$ cells per well were seeded into 96-well plates in α-MEM medium containing 10% FBS, 100 ng/mL of human RANKL and 10 or 25 ng/mL of human M-CSF or/and 12 or 25 ng/mL of human IL-34. The cell culture medium was changed

every 3 days. After 10 days of culture, $TRAP^+$ multinucleated cells containing more than 3 nuclei were considered to be osteoclasts and counted manually.

2.7. Western blot analysis

The cells were collected in a RIPA buffer (10 mM Tris pH8, 1 mM EDTA, 150 mM NaCl, 1% NP40, 0.1% SDS) containing a cocktail of protease and phosphatase inhibitors: 1 mM of sodium orthovanadate, 1 mM of phenylmethylsulforyl fluoride and 1X of Protease Inhibitor Cocktail (Roche). The protein concentration was determined using a BCA (bicinchoninic acid) protein assay (Sigma Aldrich). 40 µg of total protein extracts were prepared in a Laemmli buffer (62.5 mM Tris–HCl, pH 6.8, 2% SDS, 10% glycerol, 5% 2-mercaptoethanol, 0.001% bromophenol blue) and then separated by SDS-polyacrylamide gel electrophoresis. After electrophoretic transfer, the immobilon-P membranes (Millipore, Molsheim, France) were blotted with the antibodies referenced in the reagents section. The membranes were then probed with secondary antibodies coupled with horseradish peroxidase. Antibody binding was visualized with a Pierce enhanced chemiluminescence (ECL) kit (Thermo Scientific, Illkirch, France). The luminescence detected with a Charge Couple Device (CCD) camera was quantified using the Gene Tools image analysis software (Syngene, Cambridge, United Kingdom).

2.8. Flow cytometry experiments

Human IL-34 expression was assessed by flow cytometry (Cytomics FC500; Beckman Coulter, Villepinte, France) after fixation with 4% paraformaldehyde, permeabilization with 0.5% saponin and incubation with PE conjugated anti-human IL-34 antibody for 30

min on ice. IL-34 expression was analyzed using the CXP Analysis software 2.2 (Beckman Coulter).

2.9. ELISA assay

M-CSF released into the culture medium was quantified using a Duoset ELISA assay (R&D Systems, Abingdon, UK) according to the manufacturer's instructions. All measurements were performed in triplicate and the mean values were used in this study.

2.10. RNA isolation and real-time PCR

Total RNA was extracted using NucleoSpin® RNAII (Macherey Nagel, Duren, Germany) or TRIzol reagent (Life Technologies) with a step of DNase I treatment (25 units, 15 min) to prevent genomic contamination. One microgram of total RNA was used for first strand cDNA synthesis using the ThermoScript RT-PCR System (Invitrogen). Real-time PCR was performed from 20 ng of reverse transcribed total RNA (cDNA), 300 nM of primers and 2x SYBR Green Supermix (Biorad, Marnes-la-Coquette, France). Quantitative PCRs (qPCR) were carried out on a Bio-Rad CFX™ System (Biorad, Marnes-la-Coquette, France). Analyses were performed according to the method described by Hellemans and Vandesompele [22] and Bustin *et al*. [23] using both human and mouse hypoxanthine guanine phosphoribosyl transferase 1 (HPRT1) as invariant controls. Standard / calibration curves were produced using decreasing quantities of cDNA to validate the primers and determine their efficiency, according to the MIQE guidelines [24]. The sense and antisense primers used are as follows (human HPRT forward:

TGACCTTGATTTATTTATTTTGCATACC, reverse: CGAGCAAGACGTTCAGTCCT; mouse HPRT forward TCCTCCTCAGACCGCTTTT, reverse CCTGGTTCATCATCGCTAATC; human IL-34 forward: AATCCGTGTTGTCCCTCTTG, reverse: CAGCAGGAGCAGTACAGCAG; human M-CSF forward: GTTTGTAGACCAGGAACAGTTGAA, reverse CGCATGGTGTCCTCCATTAT; mouse IL-34 forward GGACACACTTCTGGGGACA, reverse: CCAAAGCCACGTCAAGTAGG; mouse M-CSF forward ACACCCCAATGCTAACG, reverse TGGAAAGTTCGGACACAGG; mouse M-CSFR forward ATGCTAGGACCCAGCCTGA, reverse CCTGACTGGAGAAGCCACTG).

2.11. Surface plasmon resonance assay

Experiments were carried out on a BIAcore 3000 instrument (Biacore, Uppsala, Sweden). Recombinant human M-CSF (5 µg/mL, in sodium acetate buffer pH=4.0) was covalently immobilized at a flow rate of 5 µl/min in the dextran matrix of a CM5 sensor chip (BIAcore) previously activated with an ethyl(dimethylaminopropyl) carbodiimide/ N-hydroxysuccinimide mixture. M-CSF was immobilized in a range of 200 RU (Resonance Units) and residual reactive sites were inactivated with ethanolamine pH=8.5 for 7 min. Binding assays were performed at 25°C in 10 mM Hepes buffer, pH 7.4, containing 0.15M NaCl and 0.005% P20 surfactant (HBS-P buffer, BIAcore) at a flow rate of 30 µl/min for all steps. A 1:2 serial dilution of recombinant human M-CSFR was done (from 50 nM to 0.78 nM) to validate the chip. Then, an increasing dose of recombinant human IL-34 (15.6; 31.25; 62.5; 125; 250; 500 nM) was tested for M-CSF/IL-34 binding. A regeneration step was made with a glycine buffer (10 mM pH=1.5) for 1min between each step, and 50 nM

recombinant human M-CSFR was assessed at the end to test whether the chip was still functional. The resulting sensorgrams were fitted using BiaEval 4.1 software.

2.12 Molecular docking studies of IL-34 binding to M-CSF

The three-dimensional coordinates for IL-34 were extracted from the structure published by Ma *et al*. (PDB ID: 4DKD) [15]. The coordinates for M-CSF and its receptor were extracted from the crystal structure proposed by Chen *et al*. (PDB ID: 3EJJ) [25]. The charges and atom types were assigned using the CHARMm force field [26]. IL-34 and M-CSF binding were assessed using the ZDOCK [27, 28] protein-protein docking software. The best 2000 poses were re-scored using ZRANK, a scoring function with detailed and weighted electrostatics, van der Walls and desolvation terms [29], and then clustered with an RMSD cutoff of 1 nm. As recommended, starting structures for the ligand protein were displaced from the near-native structure [27]. A representative member of the most populated cluster with the highest ZSCOREs was selected to illustrate the most favorable binding mode predicted. All calculations were executed on Pipeline Pilot 8.5 and analyses were performed using Accelrys Discovery Studio 3.5 (San Diego, CA, USA).

2.13. Confocal microscopy experiments

Cells were cultured in a plastic chamber on microscope glass slides (Millicell EZ Slide, Millipore, Billerica, MA, USA) as described above. Slides were coated using type I collagen for better spreading of the HEK cells. The cells were washed in PBS, fixed in 4% paraformaldehyde for 10 min at room temperature, permeabilized with triton X-100 0.1%

for 20 min and incubated with a blocking solution [BSA 1% with 1% of non-immune goat serum (Dako, Les Ulis, France) and 0.05% triton] for 30 min at room temperature. The cells were incubated with either the primary antibody against M-CSFR (1/200) or the blocking solution as the negative control for 90 min at 37°C. After washings, Alexa Fluor 488 secondary antibody (1/200) was added for 60 min at room temperature. Actin filaments were stained using 546-conjugated phalloidin and nuclei stained with DAPI or Draq5.

For the PLA assay, the blocking solutions used were BSA 1% with 5% of non-immune goat or donkey serum, or a mixture of both (Dako) and 0.1% triton. The cells were incubated with a rabbit anti-hM-CSF antibody (1/30) and a mouse anti-hIL-34 antibody (1/50) for 90 min at 37°C. The experiment was performed following Olink's instructions. Several negative controls were carried out: (i) PLA probes alone (no primary antibodies, addition of the blocking solution); (ii) a mixture of the two PLA probes (rabbit plus and mouse minus or rabbit minus and mouse plus) after incubation with only one of the primary antibodies to check for any cross-reactivity and non-specific signals; (iii) incubation of all antibodies on the MG-63 parental cells. All the controls were perfectly negative. Two positive controls were used: MG-63 cells (parental or 2A8 clone) incubated with the rabbit anti-hM-CSF or mouse anti-hIL-34 antibody before the two rabbit/mouse PLA probes (plus and minus). These two controls gave a signal in agreement with the results obtained with conventional immunocytostaining. Slides were mounted with liquid Prolong Gold antifade reagent (Life technologies). The slides were then observed under a confocal Nikon A1 R Si microscope using a 60X NA 1.4 oil objective and the acquisitions were obtained with NIS Element (Nikon, Champigny Sur Marne, France) at room temperature. Data were then processed with FIJI software and converted to 8bit images (ImageJ, from NIH Institute,

Bethesda, Maryland, USA). A Z-project was made with a maximal intensity projection. Smooth and sharpened functions were used, and brightness and contrast were adjusted in a same way for all conditions. The channels were then merged using the FIJI function.

2.14. Statistical analysis

Results were analyzed using GraphPad Prism 4.0 software (GraphPad Software, La Jolla, CA, USA). Non-parametric one-way analysis of variance (Kruskal–Wallis) was done, followed by a Dunn's *post hoc* test. Results are given as mean ± SEM, and results with $p<0.05$ were considered significant.

3. RESULTS

3.1. M-CSF and IL-34 induced dual additive and competitive biological effects

As M-CSF and IL-34 were considered as competitive cytokines in the literature [6], we first investigated the effects of M-CSF and IL-34 alone or in combination on the M-CSFR signaling pathways. As expected, M-CSF and IL-34 induced phosphorylation of the M-CSFR in a dose-dependent manner in HEK M-CSFR as well as the downstream signaling protein ERK1/2 (Figure 1A, B). The combination of both cytokines differentially regulated the M-CSFR signaling compared to a single dose of M-CSF or IL-34. Interestingly, when 10 ng/mL of IL-34 or M-CSF were mutually added to low doses of both cytokines, we observed an additive effect as revealed by an increased level of M-CSFR phosphorylation compared to the cytokines alone (Figure 1A, B). Similarly, this additive effect was observed for ERK1/2 in the presence of 25 ng/mL of M-CSF and 10 ng/ mL of IL-34 (Figure 1A) or 10 ng/mL of M-CSF and 25 ng/ mL of IL-34 (Figure 1B) compared to single treatments. The competitive effects previously described between M-CSF and IL-34 were observed at the higher concentrations, as shown for instance by decreased phosphorylation on M-CSFR tyrosine residues and on ERK1/2 when 10 ng/mL of M-CSF were added to 100 or 200 ng/mL IL-34 on HEK M-CSFR cells (Figure 1B).

In the light of these observations, we analyzed the biological impact of the addition of both cytokines on human $CD14^+$ monocytes (Supplementary Figure 1) and TF-1 M-CSFR cell viability (Figure 2). Consistent with previous findings [6], IL-34 and M-CSF similarly increased $CD14^+$ cell viability in a dose-dependent manner (Supplementary Figure 1A). Taken individually, the combination of 5 ng/mL M-CSF and 5 ng/mL IL-34

led to higher viability than an equivalent cumulated dose (10 ng/mL) of IL-34 but not of M-CSF (Supplementary Figure 1B). In addition, as shown previously [8], M-CSF and IL-34 similarly induced RANKL-associated osteoclastogenesis in a dose-dependent manner and the combination of M-CSF and IL-34 did not reveal any competitive or additive activity between these cytokines (Supplementary Figure 2). Both cytokines significantly up-modulated the proliferation of M-CSFR overexpressing TF-1 cells (TF-1 M-CSFR) (Figure 2A). As with the experiment conducted with $CD14^+$ cells, a combination of 5 ng/mL of each cytokine induced significantly higher proliferation compared to 10 ng/mL of M-CSF alone, whereas this difference was not significant compared to 10 ng/mL of IL-34 (Figure 2B, $p<0.05$). Addition of a blocking anti-M-CSF antibody reduced the proliferation of TF-1 M-CSFR cells, thus revealing autocrine M-CSF production by the cells (Figure 2C). This autocrine expression of M-CSF was confirmed by RT-qPCR and ELISA (Data not shown). Interestingly, this blocking anti-M-CSF antibody also decreased IL-34-induced cell proliferation with 25 ng/mL of the cytokine (Figure 2C, $p < 0.05$), and strongly reduced the modulation of ERK1/2 phosphorylation induced by IL-34 (Figure 2D). As with the TF-1 cells, HOS M-CSFR produced M-CSF in an endogenous manner (Data not shown). We then studied the contribution of autocrine M-CSF on IL-34-induced M-CSFR activation by a silencing RNA approach targeting M-CSF (Figure 3, Supplementary Figure 3A). M-CSF expression was down-regulated by around 50% 48 hours after transfections of siRNA targeting the M-CSF gene (Supplementary Figure 3A), and the silencing of M-CSF expression decreased M-CSFR phosphorylation induced by 50 ng/mL of IL-34 (Figure 3). However, high concentration of either M-CSF or IL-34 (200 ng/mL) appeared to override

cell-derived M-CSF in M-CSFR activation (Supplementary Figure 3B). Overall, these data demonstrated that combinations of both cytokines are not restricted to competitive activities, and that IL-34 and M-CSF can exhibit additive effects on various cells at certain concentrations. In addition, M-CSF is able to modulate intracellular signaling induced by IL-34 through the M-CSFR.

3.2. IL-34 can interact with the M-CSF to form a heteromeric cytokine

Because the modulation of autocrine production of M-CSF affects the M-CSFR activation induced by IL-34, we analyzed the potential molecular interaction between both cytokines by surface plasmon resonance. The sensorgrams shown in Figure 4A demonstrate the specific binding of IL-34 to immobilized M-CSF, characterized by rapid dissociation. Thus, IL-34 bound M-CSF with a low affinity (K_D=114nM) (Figure 4B). Molecular modeling based on the crystal structures published for the M-CSF, M-CSFR [13] and IL-34 [15] illustrated the conventional binding of the homodimeric cytokines on the M-CSFR (Figure 4C). A docking binding analysis was performed using the human dimer of IL-34 against the humanized structure of M-CSF derived from the mouse crystal structure. The docking strategy consisted in defining M-CSF as the rigid molecule, thus keeping its position fixed, and applying rotations and translations in the three-dimensional space for a total of 54000 docking energy evaluations, called poses. The best 2000 poses according to ZSCORE (determined using ZDOCK) were clustered to regroup similar orientations. In these clusters, the most common dimer-dimer interface was found to be a parallel orientation of IL-34 along M-CSF, with beta-strands on both cytokines arranged on the same side. The

first and most populated cluster was made of 82 structures and contained the best pose (Figure 4D, left panel). The binding interface was made of 56 amino acids on M-CSF and 47 on IL-34, for a total interface surface of 1764 Å. For each dimer, the loss in accessible solvent was of 1680 Å and 1845 Å for M-CSF and IL-34 respectively, indicating the stronger binding role of IL-34 in the resulting binding interface. The binding interface consisted of 14 hydrogen bonds between dimers and 9 salt bridges, and a detailed energy analysis of their binding mode revealed a balanced contribution of electrostatic interactions and hydrophobic contacts (data not shown). To see whether the heteromeric cytokine identified in this study can engage M-CSFR pathway activation, we explored whether the already-described binding sites for IL-34 and M-CSF could still be accessible for binding to the M-CSFR. As presented in Figure 4D (right panel), despite a steric hindrance due to its large size, the heteromeric cytokine was able to bind to the M-CSFR, leading to a different conformation of the intracellular M-CSFR chains. In this conformation, one of the two cytokine binding sites remained accessible to the M-CSFR and the two free sites were opposite each other on the tetrameric cytokine. If we superimposed two M-CSFR monomers on the predicted dimer of dimers, the resulting orientation for each M-CSFR monomer was compatible with the estimated distance between the missing D4 and D5 domains of the two M-CSFR monomers. This distance was a critical step for receptor activation as it allowed contact between the two D4 monomers *via* homotypic contacts [19]. M-CSF and IL-34 can thus form a heteromeric cytokine able to bind to the M-CSFR.

3.3. Endogenous M-CSF and IL-34 can interact together within the cell cytoplasm

As M-CSF and IL-34 were predicted to form a heteromeric cytokine, we further investigated by means of a PLA assay whether such interaction could be relevant in cells producing both cytokines (Figure 5). We developed from the parental MG63 cell line (MG63 NT) that intrinsically expressed M-CSF but not IL-34, a transfected MG63 IL-34 cell line that expressed both M-CSF and IL-34 at the protein level, as demonstrated by the pink staining around the nuclei compared to the negative controls (Figure 5A,B). The PLA assay demonstrated molecular interaction between the two cytokines as shown by pink fluorescent points within the cytoplasm in Figure 5C, characterized by a close proximity of the protein epitopes (30-40nm).

3.4. Endogenous M-CSF and IL-34 expression differentially control intracellular trafficking and maturation of the M-CSFR

M-CSFR half-life was analyzed in the presence of M-CSF or IL-34 in HEK cells expressing the M-CSFR. As expected, HEK M-CSFR cell lysates revealed two forms of M-CSFR, the higher molecular form corresponding to the membrane form of the receptor (Figure 6). Adding M-CSF or IL-34 decreased the membrane expression of M-CSFR, thus reflecting the receptor's internalization and degradation as protein synthesis was blocked by cycloheximide. At the same dose, M-CSF was more efficient in reducing the half-life of the M-CSFR compared to IL-34 (Figure 6A). When M-CSF was overexpressed concomitantly to the M-CSFR, the cytokine markedly down-regulated the expression of the membrane form of its receptor in favor of the intracellular form (Figure 6B). On the contrary, the M-CSFR was maintained at the cell membrane when IL-34 was co-transfected (Figure 6B). As

with HEK M-CSFR cells, overexpression of M-CSF in HOS M-CSFR cells quantitatively increased the intracellular form and decreased the membrane form of the receptor in contrast to IL-34 overexpression, which maintained receptor expression at the cell membrane (Supplementary Figure 4). Non-transfected HOS M-CSFR and HEK M-CSFR cells or cells transfected with an empty vector (Mock) mainly expressed the receptor at the membrane (Figure 6B, Supplementary Figure 4). A trypsin treatment of HEK M-CSFR cells was associated with the formation of degradation products of the M-CSFR in contrast with the M-CSF co-expressing cells (Figure 6C). These results demonstrated that the upper band (175 kDa) corresponded well to the membrane form of the M-CSFR and the lower band (150 kDa) to an intracellular form. Adding tunicamycin to HEK M-CSFR cells for 24 hours or 48 hours resulted in a lower molecular weight form of the receptor, around 100 kDa corresponding to its non-N-glycosylated form, whereas brefeldin A treatment induced a total shift toward the 150 kDa M-CSFR form, similar to M-CSF co-expression (Figure 6C). As tunicamycin is known to prevent proteins' *N*-glycosylation, and brefeldin A to both interfere with transport from the endoplasmic reticulum to the Golgi apparatus and block protein secretion, the present data suggest that M-CSF treatment blocked M-CSFR trafficking in the endosomal network, leading to the accumulation of a less *N*-glycosylated form of 150 kDa (Figure 6C). However, treatment of HEK M-CSFR cells with M-CSFR ligands for 48 hours did not induce any shift between the two forms of M-CSFR, demonstrating that only intrinsic expression of M-CSF and IL-34 can impact receptor maturation (Figure 6D).

Confocal microscopy confirmed these data in HEK M-CSFR (Figure 7) and HOS M-CSFR cells (Supplementary Figure 5). M-CSF overexpression induced marked

intracellular sequestration of the M-CSFR that appeared located in the perinuclear region (Figure 7, Supplementary Figure 5). Overexpression of IL-34 led to minor intracellular sequestration of the receptors as they were still localized at the cell membrane. Moreover, co-expression of M-CSF and IL-34 mainly led to intracellular expression of the M-CSFR clustered in the endosomal network around the nuclei (Figure 7, Supplementary Figure 5), confirming the Western blot observations (Data not shown). Similar investigations were performed in the murine osteosarcoma cells K7M2 that spontaneously expressed M-CSF and IL-34 (Supplementary Figure 6). Supplementary Figure 6 shows a main intracellular localization of the M-CSFR with slight expression of its membrane form. Western blot analysis confirmed the expression of both M-CSFR forms with a relatively high expression of the intracellular form compared to HEK M-CSFR (Figure 6) or HOS M-CSFR (Supplementary Figure 4). Overall, these data demonstrate that intrinsic IL-34 and M-CSF expression controls cellular trafficking of the M-CSFR.

4. DISCUSSION

Despite common features, previous studies described specific activities for M-CSF and IL-34, especially in their ability to modulate the expression of various chemokines/chemokine receptor expression (monocyte chemoattractant protein-1 MCP-1, eotaxin-2, C-C chemokine receptor type 2 CCR2), and the migration of myeloid cells through their shared M-CSFR chains [11, 30]. In the present work, we report for the first time the molecular interaction between M-CSF and IL-34, forming a new heteromeric cytokine, and the differential role of M-CSFR ligands in controlling M-CFSR trafficking. Furthermore, the M-CSF/IL-34 heteromer may play a specific biological role by differentially phosphorylating the M-CSFR due to the tridimensional conformation of the receptor chains adopted when the cytokines bind. ZDOCK docking software was used to look for an interaction between M-CSF and IL-34, as it is particularly efficient on dimeric proteins, while finding the correct interface from two monomers to form a dimer. We first explored whether the docking followed by clustering strategy could be useful for studying existing binding interfaces of the M-CSFR ligands by isolating each cytokine from its receptor or by splitting dimers into monomers. Each docking assessment found the correct position and orientation in the first populated and most energy favorable cluster, even in the case of the M-CSF molecule where the disulfide bridge could not be created during the docking process. Without the *N*-glycosylations present in the IL-34 structures, we also observed aggregation-like motifs, a phenomenon already identified experimentally [12]. There was no defined orientation or specific binding interfaces that could be deduced from the aggregated dimers. However, the same studies on M-CSF dimers did not reproduce any

aggregation pattern, which was also a good indicator of the sensitivity of the methods used. These validations reinforced our confidence in the docking protocol used for studying the putative binding mode of the cytokines. The *in silico* experiments revealed a potential binding mode for M-CSF and IL-34 dimers (Figure 4D), arranged parallel to each other with their beta-strands pointing in the same direction. This striking binding mode was unexpected so we first decided to rule out the possibility that the results obtained were only due to the docking strategy or algorithm employed. We therefore used another popular rigid protein docking algorithm called PIPER *via* its web-based interface ClusPro, which best performed recently in the latest CAPRI contest [31, 32]. By using dimers of dimers as starting structures we also found a parallel orientation for both cytokines. Consistent with this docking study, surface plasmon resonance assays experimentally validated the binding ability of IL-34 to the M-CSF characterized by low affinity and rapid dissociation (Figure 4A). The proximity ligation assay confirmed their interaction. Indeed, this technique made it possible to detect closed epitopes separated by a maximum distance of around 30-40 nm [33], and finally strengthened the binding between both in their physiological context (Figure 5). This heteromeric cytokine may be stabilized by its binding to the M-CSFR, as the molecular docking study proposed a new binding mode for this heteromeric cytokine to two isolated M-CSFR chains (Figure 4D). This recruitment could bring each M-CSFR domain D3 to a distance of about 60Å, close enough to bring domains D4 and D5 into contact, a step known to be critical for receptor activation [17-19].

The oligomerization process is widespread in biology and it is estimated that homo-oligomerization occurs with 70% of eukaryotic proteins [34]. Increased efficiency made

possible by better stability, amplification of their affinity or the protective mechanisms of the proteins are amongst the main benefits of this oligomerization process. By forming homodimers, M-CSFR, M-CSF and IL-34, like numerous other cytokines/receptors, do not break this oligomerization rule [35]. To increase the complexity, diversity and regulation of cell signaling events, several cytokines are able to form heteromeric structures. This is the case of interleukin-12 (IL-12) related cytokines which differentially regulate the maintenance or activation of the Th1 immune response [36]. Similarly to IL-12, IL-17A and IL-17F, two members of the IL-17 family, also interact to form a heterodimer able to bind to the IL-17RA/IL-17RC receptor complex [37].

Based on our data, M-CSF and IL-34 now belong to the cytokine families forming heteromeric entities and the M-CSF/IL-34 cytokine plays a part in increasing the functional diversity of these molecules. By interfering with M-CSFR trafficking, more specifically in the balance between the intracellular and membrane forms of the receptor, IL-34, M-CSF and M-CSF/IL-34 may tightly and specifically control the biological activities associated with the M-CSFR-dependent signaling pathways. In M-CSFR expressing cells, overexpression of M-CSF led preferentially to maintaining the M-CSFR in an *N*–glycosylated form clusterized into the endosomal network. Western blot carried out in these experimental conditions showed a shift in M-CSFR expression from the high molecular weight of 175 kDa, corresponding to the membrane mature form of the receptor, to the 150 kDa intracytoplasmic form. These results were consistent with previous studies which demonstrated that the 175 kDa membrane form was highly processed and modified with mannose and sialic acid, whereas the 150 kDa form was less mature with only mannose

modifications, and accumulated in the Golgi apparatus, a process called receptor maturation arrest [38-40]. The tunamycin treatment, which is known to prevent the glycosylation process [41], and brefeldin A treatment, which blocks anterograde transport from the endoplasmic reticulum to the Golgi apparatus and protein secretion [42, 43], confirm that the M-CSFR form processed when M-CSF is highly expressed by the cells is less glycosylated compared to the mature form, and that the receptor is retained between the endoplasmic reticulum and the Golgi apparatus. In contrast, co-expression of IL-34 did not induce massive intracellular clustering of M-CSFR and maintained the receptor at the cell surface, suggesting a different regulatory role for the twin cytokines in M-CSFR trafficking. Similar functional differences can be observed on the receptor half-life after adding exogenous cytokines (Figure 6), but also at the transcriptional level as an increase in IL-34 expression has a moderate impact on M-CSF or M-CSFR expression levels (unpublished data). In contrast, overexpression of M-CSF induces significant changes in the M-CSFR or IL-34 levels. Indeed, overexpression of M-CSF induces a significant increase in IL-34 expression, whereas overexpression of IL-34 does not modify M-CSF expression (unpublished data). In addition, knock-down of M-CSF expression using siRNA enhances IL-34 expression, suggesting a compensatory mechanism between these two cytokines. Nandi *et al.* recently published that M-CSFR and its two ligands IL-34 and M-CSF exhibit distinct expression patterns during brain development and that IL-34 exhibits a broader regional expression than M-CSF, mostly without overlap [44]. Their observations suggest a key regulatory role for IL-34 in the M-CSF/M-CSFR activation pathway, which consequently may participate to the tissue homeostasis and development. Thus, our results

show that IL-34 may modulate M-CSF effects through the M-CSFR, explained in part by the formation of a heteromeric cytokine M-CSF/IL-34. In addition to the already identified functions of IL-34 and M-CSF in exacerbated macrophage activation (bowel diseases, liver fibrosis, chronic skin inflammation, arthritis, etc), this new heteromeric cytokine M-CSF/IL-34 which may differentially regulates the activation/localisation of M-CSFR strengthens the global therapeutic approaches for blocking all biological functions coming from these molecules [7,8, 45-51].

In contrast to IL-17A or IL-17F that form either disulfide-linked homodimers or heterodimers through their cysteine knot motif, M-CSF and IL-34 probably interact in their homodimeric form to constitute a heterotetrameric cytokine. Our molecular docking studies predicted a 2:2 interaction without any disulfide bond, which is able to bind to the M-CSFR, unlike a single M-CSF/IL-34 heterodimer. The exact functional implication of this new oligomeric cytokine still needs to be explored and must now be analysed in the light of the receptor protein tyrosine phosphatase β/ζ (RPTP β/ζ) identified as a new receptor for IL-34 [44], not expressed in the $CD14^{+}$ and myeloid cells analysed in the present study [51]. The involvement of these oligomeric cytokine should be also investigated in light of syndecan-1which has been recently identified as new IL-34 effector [51]. As with the IL17A/IL17F and IL-17RA/IL-17RC systems, the heteromeric M-CSF/IL-34 may regulate IL-34 and M-CSF functions through one receptor or another and the heteromer may also interact with both M-CSFR and RPTP β/ζ receptors. This new M-CSFR cooperative binding mode needs further exploration, and the crystal structure of M-CSF/IL-34 should be determined as well as co-crystal studies with the receptors to better characterize this new complex. It remains to be understood why and in which context this heteromerization

mechanism is more beneficial than the already described one-to-one competition. In conclusion, the present work demonstrated that simultaneous addition of M-CSF and IL-34 led to a specific activation pattern on the M-CSFR, with higher phosphorylation of the tyrosine residues at low concentrations. Similarly, both cytokines showed an additive effect on cellular proliferation or viability that can be explained by the formation of a heteromeric M-CSF/IL-34 cytokine predicted by molecular docking studies. This interaction between M-CSF and IL-34 was confirmed by surface plasmon resonance and proximity ligation assays. In addition, co-expression of the M-CSFR and its ligands differentially regulates the receptor's glycosylation state and localization in the cell. This is the first report demonstrating the direct interaction between IL-34 and M-CSF and their ability to form a new heteromeric cytokine that may play a part in the tissue homeostasis and development.

ACKNOWLEDGEMENTS: The authors would like to thank Juliette Desfrançois-Noel from the cell sorting facility (Plateau de cytométrie SFR Bonamy/INSERM U892, Nantes, France) for her help in cell sorting the cells expressing the M-CSFR, and Mike Maillasson from the Plateforme IMPACT (SFR Bonamy, FED 4203/ INSERM UMS 016/CNRS 3556, Nantes, France) where the surface plasmon resonance experiments were carried out. We are especially grateful to Julien Jardin and Valérie Briard from the analytical facility at the UMR 1253 INRA/Agrocampus-Ouest (STLO Science et Technologie du Lait et de l'œuf, Rennes, France), who helped us to perform spectrometry analysis to determine M-CSF/IL-34 stoichiometry. We would also like to thank Dr Valérie Trichet (INSERM U957, Nantes, France) for her technical and rewarding advice regarding molecular cloning of the human M-CSFR gene. This study was supported by the Region des Pays de la Loire (CIMATH II research project) and by the Ligue Nationale Contre le Cancer (Equipe LIGUE 2012).

AUTHORSHIP: A.I.S., R.B. and C.C. performed cell biology and biochimistry studies. A.S. and B.B. performed P.L.A. and confocal microscopy experiments. M.M. perfomed Surface plasmon resonance experiments. S.T. performed molecular docking. D. H. and A.S. planned the work and D.H., A.S. and S.T. contributed to the manuscript.

REFERENCES

[1] Stanley ER, Chitu V. CSF-1 receptor signaling in myeloid cells. Cold Spring Harbor Pespect Biol 2014 ;6 : a021857.

[2] Dai XM, Ryan GR, Hapel AJ, Dominiguez MG, Russel RG, Kapp S, Sylverstre V, Stanley ER. Targeted disruption of the mouse colony-stimulating factor 1 receptor gene results in osteopetrosis, mononuclear phagocyte deficiency, increased primitive progenitor cell frequencies, and reproductive defects. Blood 2002;99 :111–120.

[3] Wiktor-Jedrzejczak W, Bartocci A, Ferrante AW Jr, Ahemd-Ansari A, Sell KW, Pollard JW, Stanley ER. Total absence of colony-stimulating factor 1 in the macrophage-deficient osteopetrotic (op/op) mouse. Proc Natl Acad Sci USA 1990 ;87 : 4828–4832.

[4] Yoshida H, Hayashi S, Kunisada T, Ogawa M, Nishikawa S, Okamura H, Sudo T, Shultz LD, Nishikawa S. The murine mutation osteopetrosis is in the coding region of the macrophage colony stimulating factor gene. Nature 345, 442–444.

[5] Wei S, Nandi S, Chitu V, Yeung YG, Yu W, Huang M, Williams LT, Lin H, Stanley ER. Functional overlap but differential expression of CSF-1 and IL-34 in their CSF-1 receptor-mediated regulation of myeloid cells. J Leukoc Biol 2010 ;88 : 495 –505.

[6] Lin H, Lee E, Hestir K, Leo C, Huang M, Bosch E, Halenbeck R, Wu G, Zhou A, Berhens D, Hollebaugh D, Linnemann T, Qin M, Wong J, Chu K, Doberstein SK, Williams LT. Discovery of a Cytokine and Its Receptor by Functional Screening of the Extracellular Proteome. Science 2008 ; 320 :807–811.

[7] Foucher ED, Blanchard S, Preisser L, Garo E, Ifrah N, Guardiola P, Delneste Y, Jeannin P. IL-34 Induces the Differentiation of Human Monocytes into Immunosuppressive Macrophages. Antagonistic Effects of GM-CSF and IFNγ. PloS One 2013 ;8 : e56045.

[8] Baud'Huin M, Renault R, Charrier C, Riet A, Moreau A, Brion R, Gouin F, Duplomb L, Heymann D. Interleukin-34 is expressed by giant cell tumours of bone and plays a key role in RANKL-induced osteoclastogenesis. J Pathol 2010 ; 221 : 77–86.

[9] Nandi S, Gokhan S, Dai XM, Wei S, Enikolopov G, Lin H, Mehler MF, Stanley ER. The CSF-1 receptor ligands IL-34 and CSF-1 exhibit distinct developmental brain expression patterns and regulate neural progenitor cell maintenance and maturation. Dev Biol 2012 ; 367 : 100–113.

[10] Wang Y, Szretter KJ, Vermi W, Gilfillan S, Rossini C, Cella M, Barrow AD, Diamond MS, Colonna M. IL-34 is a tissue-restricted ligand of CSF1R required for the development of Langerhans cells and microglia. Nat Immunol 2012 ; 13 : 753-760.

[11] Chihara T, Suzu S, Hassan R, Chutiwitoonchai N, Hiyoshi M, Motoyoshi K, Kimura F, Okada S. 2010 L-34 and M-CSF share the receptor Fms but are not identical in biological activity and signal activation. Cell Death Differ. 17, 1917–1927.

[12] Liu H, Leo C, Chen X, Wong BR, Williams LT, Lin H, He X. The mechanism of shared but distinct CSF-1R signaling by the non-homologous cytokines IL-34 and CSF-1. Biochim Biophys Acta 2012 ;1824 : 938–945.

[13] Pandit J, Bohm A, Jancarik J, Halenbeck R, Koths K, Kim SH. Three-dimensional structure of dimeric human recombinant macrophage colony-stimulating factor. Science 1992 ;258 : 1358–1362.

[14] Garceau V, Smith J, Paton IR, Davey M, Fares MA, Sester DP, Burt DW, Hume DA. Pivotal Advance: Avian colony-stimulating factor 1 (CSF-1), interleukin-34 (IL-34), and CSF-1 receptor genes and gene products. J Leukoc Biol 2010 ; 87 : 753–764.

[15] Ma X, Lin WY, Chen Y, Stawicki S, Mukhyala K, Wu Y, Martin F, Bazan JF, Staronasnik MA. Structural Basis for the Dual Recognition of Helical Cytokines IL-34 and CSF-1 by CSF-1R. Structure 2012;20 : 676–687.

[16] Price K, Choi HU, Rosenberg L, Stanley ER. The predominant form of secreted colony stimulating factor-1 is a proteoglycan. J. Biol. Chem 1992 ; 267, 2190-2199.

[17] Felix J, Elegheert J, Gutsche I, Shkumatov AV, Wen Y, Bracke N, Pannecouke E, Vandenberghe I, Devreese B, Svergun DI, Pauwels E, Vergauwen B, Savvides SN.

Human IL-34 and CSF-1 establish structurally similar extracellular assemblies with their common hematopoietic receptor. Structure 2013 ;21 : 528-39.

[18] Verstraete K, Savvides SN. Extracellular assembly and activation principles of oncogenic class III receptor tyrosine kinases. Nat Rev Cancer 2012 ;12:753–766.

[19] Elegheert J, Desfosses A, Shkumatov AV, Wu X, Bracke N, Verstrate K, Van Craenenbroeck K, Brooks BR, Svergun DI, Vergauwen B, Gutsche I, Savvides SN. Extracellular complexes of the hematopoietic human and mouse CSF-1 receptor are driven by common assembly principles. Structure 2011 ; 19 : 1762–1772.

[20] Reynolds A, Leake D, Boese Q, Scaringe S, Marshall WS, Khvorova A. Rational siRNA design for RNA interference. Nat Biotechnol 2004 ; 22 : 326–330.

[21] Naito Y, Ui-Tei K. Designing functional siRNA with reduced off-target effects. Methods Mol Biol 2013 ; 942 : 57–68.

[22] Hellemans J, Vandesompele J. Selection of reliable reference genes for RT-qPCR analysis. Methods Mol Biol 2014 ; 1160 : 19–26.

[23] Bustin SA, Benes V, Garson J, Hellemans J, Huggett J, Kubista M, Mueller R, Nolan T, Pfaffl MW, Shipley G, Wittwer CT, Schjerling P, Day PJ, Abreu M, Aguado B, Beaulieu JF, Beckers A, Bogaert S, Browne JA, Carrasco-Ramiro F, Ceelen L, Ciborowski K, Cornillie P, Coulon S, Cuypers A, De Brouwer S, De Ceuninck L, De Craene J, De Naeyer H, De Spiegelaere W, Deckers K, Dheedene A, Durinck K, Ferreira-Teixeira M, Fieuw A, Gallup JM, Gonzalo-Flores S, Goossens K, Heindryckx F, Herring E, Hoenicka H, Icardi L, Jaggi R, Javad F, Karampelias M, Kibenge F, Kibenge M, Kumps C, Lambertz I, Lammens T, Markey A, Messiaen P, Mets E, Morais S, Mudarra-Rubio A, Nakiwala J, Nelis H, Olsvik PA, Pérez-Novo C, Plusquin M, Remans T, Rihani A, Rodrigues-Santos P, Rondou P, Sanders R, Schmidt-Bleek K, Skovgaard K, Smeets K, Tabera L, Toegel S, Van Acker T, Van den Broeck W, Van der Meulen J, Van Gele M, Van Peer G, Van Poucke M, Van Roy N, Vergult S, Wauman J, Tshuikina-Wiklander M, Willems E, Zaccara S, Zeka F, Vandesompele J. The need for transparency and good practices in the qPCR literature. Nat Methods 2013 ; 10 : 1063–1067.

[24] Huggett JF, Foy CA, Benes V, Emslie K, Garcon JA, Haynes R, Hellemans J, Kubista M, Mueller RD, Nolan T, Pfaffl MW, Shipley GL, Vandesompele J, Wittwer CT, Bustin

SA. The digital MIQE guidelines: Minimum Information for Publication of Quantitative Digital PCR Experiments. Clin Chem 2013 ; 59 : 892–902.

[25] Chen R, Weng Z. Docking unbound proteins using shape complementarity, desolvation, and electrostatics. Proteins 2002 ; 47 : 281–294.

[26] Momany FA, Rone R. Validation of the general purpose QUANTA ®3.2/CHARMm® force field. J Comput Chem 1992 ; 13 : 888–900.

[27] Chen X, Liu H, Focia PJ, Shim AHR, He X. Structure of macrophage colony stimulating factor bound to FMS: diverse signaling assemblies of class III receptor tyrosine kinases. Proc Natl Acad Sci USA 2008 ; 105 : 18267–18272.

[28] Li L, Chen R, Weng Z. RDOCK: refinement of rigid-body protein docking predictions. Proteins 2003 ;53 :693–707.

[29] Pierce B, Weng Z. ZRANK: reranking protein docking predictions with an optimized energy function. Proteins 2007 ;67 : 1078–1086.

[30] Barve BA, Zack MD, Weiss D, Song RH, Beidler D, Head RD. 2013 Transcriptional profiling and pathway analysis of CSF-1 and IL-34 effects on human monocyte differentiation. Cytokine 63, 10–17.

[31] Kozakov D, Beglov D, Bohnuud T, Mottarella SE, Xia B, Hall DR, Vajda S. 2013 How good is automated protein docking? Proteins 81, 2159–2166.

[32] Kozakov D, Brenke R, Comeau SR, Vajda S. IPER: an FFT-based protein docking program with pairwise potentials. Proteins 2006 ;65 : 392–406.

[33] Söderberg O, Gullberg M, Jarvius M, Ridderstråle K, Leuchowius KJ, Jarvius J, Wester K, Hydbring P, Bahram F, Larsson LG, Landegren U. Direct observation of individual endogenous protein complexes in situ by proximity ligation. Nat Methods 2006 ;3 : 995–1000.

[34] Goodsell DS, Olson AJ. Structural symmetry and protein function. Annu Rev Biophys Biomol Struct 2000 ; 9 : 105–153.

[35] Atanasova M, Whitty A. Understanding cytokine and growth factor receptor activation

mechanisms. Crit Rev Biochem Mol Biol 2012 ; 47 : 502–530.

[36] Gately MK, Renzetti LM, Magram J, Stern AS, Adorini L, Gubler U, Presky DH. The interleukin-12/interleukin-12-receptor system: role in normal and pathologic immune responses. Annu Rev Immunol 1998 ;16 : 495–521.

[37] Toy D, Kugler D, Wolfson M, Vanden Bos T, Hurgel J, Derry J, Tocker J, Peschon J. Interleukin 17 Signals through a Heteromeric Receptor Complex. J Immunol 2006;177; 36–39.

[38] Kawasaki ES, Ladner MB. Molecular biology of macrophage colony-stimulating factor. Immunol Ser 1990;49: 155–176.

[39] Hassan R, Suzu S, Hiyoshi M, Takahashi-Makise N, Ueno T, Agatsuma T, Akari H, Komano J, Takebe Y, Motoyoshi K, Okada S. Dys-regulated activation of a Src tyroine kinase Hck at the Golgi disturbs N-glycosylation of a cytokine receptor Fms. J Cell Physiol 2009; 221: 458–468.

[40] Hiyoshi M, Suzu S, Yoshidomi Y, Hassan R, Harada H, Sakashita N, Akari H, Motoyoshi K, Okada S. Interaction between Hck and HIV-1 Nef negatively regulates cell surface expression of M-CSF receptor. Blood 2008;111: 243–250.

[41] Price NPJ, Tsvetanova B. Biosynthesis of the tunicamycins: a review. J Antibio 2007; 60: 485–491.

[42] Nebenführ A, Ritzenthaler C, Robinson DG. Brefeldin A: Deciphering an Enigmatic Inhibitor of Secretion. Plant Physiol 2002;130: 1102–1108.

[43] Verbert A, Cacan R. Trafficking of oligomannosides released during N-glycosylation: a clearing mechanism of the rough endoplasmic reticulum. Biochim Biophys Acta 1999; 1473: 137–146.

[44] Nandi S, Cioce M, Yeung YG, Nieves E, Tesfa L, Lin H, Hsu AW, Halenbeck R, Cheng HY, Gokhan S, Mehler MF, Stanley ER. Receptor-type protein-tyrosine phosphatase ζ is a functional receptor for interleukin-34. J Biol Chem 2013; 288: 21972–21986.

[45] Masteller EL, Wong BR. Targeting IL-34 in chronic inflammation. Drug Discov Today, 2014 19 (8), 1212-1216.

[46] Yamane F, Nishikawa Y, Matsui K, Asakura M, Iwasaki E, Watanabe K, Tanimoto H, Sano H, Fujiwara Y, Stanley ER, Kanayama N, Mabbott NA, Magari M, Ohmori H. CSF-1 receptor-mediated differentiation of a new type of monocytic cell with B cell-stimulating activity: its selective dependence on IL-34. J Leukoc Biol, 2014 95(1):19-31.

[47] Chemel M, Le Goff B, Brion R, Cozic C, Berreur M, Amiaud J, Bougras G, Touchais S, Blanchard F, Heymann MF, Berthelot JM, Verrecchia F, Heymann D. Interleukin 34 expression is associated with synovitis severity in rheumatoid arthritis patients. Ann Rheum Dis, 2012 71(1):150-154.

[48] Preisser L, Miot C, Le Guillou-Guillemette H, Beaumont E, Foucher ED, Garo E, Blanchard S, Frémaux I, Croué A, Fouchard I, Lunel-Fabiani F, Boursier J, Roingeard P, Calès P, Delneste Y, Jeannin P. IL-34 and macrophage colony-stimulating factor are overexpressed in hepatitis C virus fibrosis and induce profibrotic macrophages that promote collagen synthesis by hepatic stellate cells. Hepatology, 2014 60(6):1879-1090.

[49] Franzè E, Monteleone I, Cupi ML, Mancia P, Caprioli F, Marafini I, Colantoni A,

Ortenzi A, Laudisi F, Sica G, Sileri P, Pallone F, Monteleone G. Interleukin-34 sustains inflammatory pathways in the gut. Clin Sci, in press.

[50] Fend L, Accart N, Kintz J, Cochin S, Reymann C, Le Pogam F, Marchand JB, Menguy T, Slos P, Rooke R, Fournel S, Bonnefoy JY, Préville X, Haegel H. Therapeutic effects of anti-CD115 monoclonal antibody in mouse cancer models through dual inhibition of tumor-associated macrophages and osteoclasts. PLoS One, 2013 8(9):e73310.

[51] Ségaliny AI, Brion R, Mortier E, Maillasson M, Cherel M, Jacques Y, Le Goff B, Heymann D. Syndecan-1 regulates the biological activities of interleukin-34. Biochemica Biophysica Acta Mol Cell Res, 2015 1853(5):1010-1021

Figure Legends

Figure 1: M-CSF and IL-34 alone or in combination differentially activate the M-CSFR. Tyrosine phosphorylation patterns (P-Tyr$_{708}$, P-Tyr$_{723}$, and P-Tyr$_{923}$) for M-CSFR and Erk1/2 phosphorylation were investigated by Western blot after 5 min of cytokine addition to the cells. (**A**) HEK M-CSFR cells were cultured in serum-free conditions for 12h before stimulation for 5 min at 37°C with increasing doses of M-CSF (10, 25, 50, 100 and 200 ng/mL) combined or not with 10 ng/mL of IL-34. (**B**) Similarly, HEK M-CSFR cells were incubated with increasing concentrations of IL-34 (10, 25, 50, 100 and 200 ng/mL) with or without 10 ng/mL of M-CSF. β-actin was used as the loading control. Bar graphs show relative densitometric values of pTyr-708 an pERK1/2 normalised to β-actin and to the control (CT) condition.

Figure 2: Autocrine production of M-CSF modulates the biological effects of IL-34. **(A)** TF-1 M-CSFR cells were cultured in the presence or absence of M-CSF or IL-34 for 3 days. Cell number was counted manually and histograms represent the percentage of proliferation compared to the control group. Original magnification: X100. (**B**) TF-1 M-CSFR cells were cultured in the presence or absence of M-CSF or IL-34 or both cytokines at 5 ng/mL for 7 days. Cell proliferation was quantified by manual counting and histograms illustrate the percentage of proliferation compared to D0 and normalized to the 5 ng/mL M-CSF condition. (**C**) 10^4 cells/well were seeded in 96-well plates and cultured with or

without M-CSF or IL-34 in the presence or absence of a blocking anti-M-CSF antibody. After 3 days of culture, cell viability was determined by an Alamar blue assay. (**D**) TF-1 M-CSFR cells were cultured in serum free conditions for 12 hours before incubation with a blocking anti-M-CSF antibody. The cells were then stimulated with M-CSF or IL-34 for 5 min and the level of P-ERK1/2 was studied by Western blot. β-actin was used as the loading control. Error bars show the SEM for three different experiments. *$p < 0.05$, ** $p < 0.01$, *** $p < 0.001$.

Figure 3: Blockade of M-CSF cell expression decreases IL-34-induced M-CSFR activation. HOS M-CSFR cells were transfected with siRNAs directed against the human M-CSF gene (siM-CSF$_{621}$, siM-CSF$_{778}$, siM-CSF$_{952}$). An siRNA directed against the luciferase gene (siLucF) was used as a control. Forty-eight hours after transfection, the cells were cultured in serum-free conditions for 12 hours and then stimulated with 50 ng/mL of M-CSF or IL-34 for 5 min. Tyrosine$_{708}$ and tyrosine$_{723}$ phosphorylation of the M-CSFR were studied by Western blot. β-actin was used as the loading control. The phosphorylation density of the tyrosine$_{723}$ was quantified using GeneTools (Syngene) and normalized to the β-actin density.

Figure 4: IL-34 binds M-CSF to form a heterodimeric protein able to interact with the M-CSFR. (**A**) M-CSF was immobilized on the dextran matrix of a sensor chip (BIAcore) and increasing doses of IL-34 (from 15.575 to 500 nM) were loaded on to the chip to analyze the interactions between the 2 cytokines. (**B**) Figure representing dose-dependent

binding in RU and shows dissociation constant (K_D) determination. (**C**) Molecular modeling was performed on the homodimeric cytokines in complex with the M-CSFR using the three-dimensional coordinates extracted from the crystal structure previously published. (**D**) The interactions between M-CSF and IL-34 were assessed by molecular modeling using three-dimensional cytokine structures. The left panel shows the most favorable binding mode between the two homodimeric cytokines, and the right panel illustrates interaction between the heteromeric cytokine and the M-CSFR. M-CSF in brown, IL-34 in green and M-CSFR in blue.

Figure 5: M-CSF and IL-34 interact within the cytoplasm of cells expressing both cytokines. (**A**) First, the proximity ligation assay (PLA) from Olink was used to detect M-CSF and IL-34 expression (far red, represented in pink) in MG63 cell lines (MG63 NT only express M-CSF, and MG63 IL-34 cells express both cytokines). Nuclei were stained with DAPI (cyan). (**B**) Several negative controls were performed on MG63 IL-34 cells to validate the PLA assays: cells incubated with only one primary antibody (either against M-CSF or IL-34) and both secondary antibodies, or with only secondary antibodies; MG63 NT cells incubated with all the antibodies. (**C**) In situ PLA showed the co-localization of M-CSF and IL-34 in the cytoplasm of MG63 IL-34 cells (pink staining). Cell morphology was analyzed using digital interference reflection images captured using the reflection mode (gray).

Figure 6: M-CSF and IL-34 differentially control the intracellular trafficking of the M-CSFR. (**A**) HEK M-CSFR cells were treated with 4 µg/mL of cycloheximide to block

protein synthesis in the presence or absence of 100 ng/mL of M-CSF or IL-34. M-CSFR expression was followed by Western blot after 2, 4, 6 or 8 hours of treatment and quantified compared to β-actin expression. (**B**) HEK M-CSFR were transfected with a vector encoding M-CSF or IL-34 or with an empty vector as control and 48 hours later, M-CSFR and ERK1/2 phosphorylation was assessed by Western blot. (**C**) M-CSFR expression analyzed by Western blot. HEK M-CSFR cells transfected for expressing M-CSF ("M-CSF") or transfected with an empty vector ("Control") were treated 48 hours after transfection with PBS or trypsin (0.05%) for 10 min at 37°C. Non-transfected HEK M-CSFR cells ("NT") were treated for 24 or 48 hours with tunicamycin and brefeldin which block the glycosylation process and the protein export between the reticulum and the Golgi networks respectively. (**D**) HEK M-CSFR cells were cultured with 25 ng/mL of M-CSF or IL-34 for 48 hours prior to analyze the M-CSFR, and P- Erk1/2 by Western blot. β-actin was used as the loading control.

Figure 7: M-CSF and IL-34 co-expression induces intracellular sequestration of the M-CSFR in HEK M-CSFR cells. HEK M-CSFR cells were transfected with an empty vector (Mock), a vector coding for M-CSF (M-CSF) or IL-34 (IL-34) or co-transfected with both vectors encoding M-CSF and IL-34 (M-CSF/IL-34). Forty-eight hours after transfection, the cells were fixed and the expression of M-CSFR was assessed by confocal microscopy (green staining). Actin is stained in red, and nuclei are shown in blue.

Figure 1

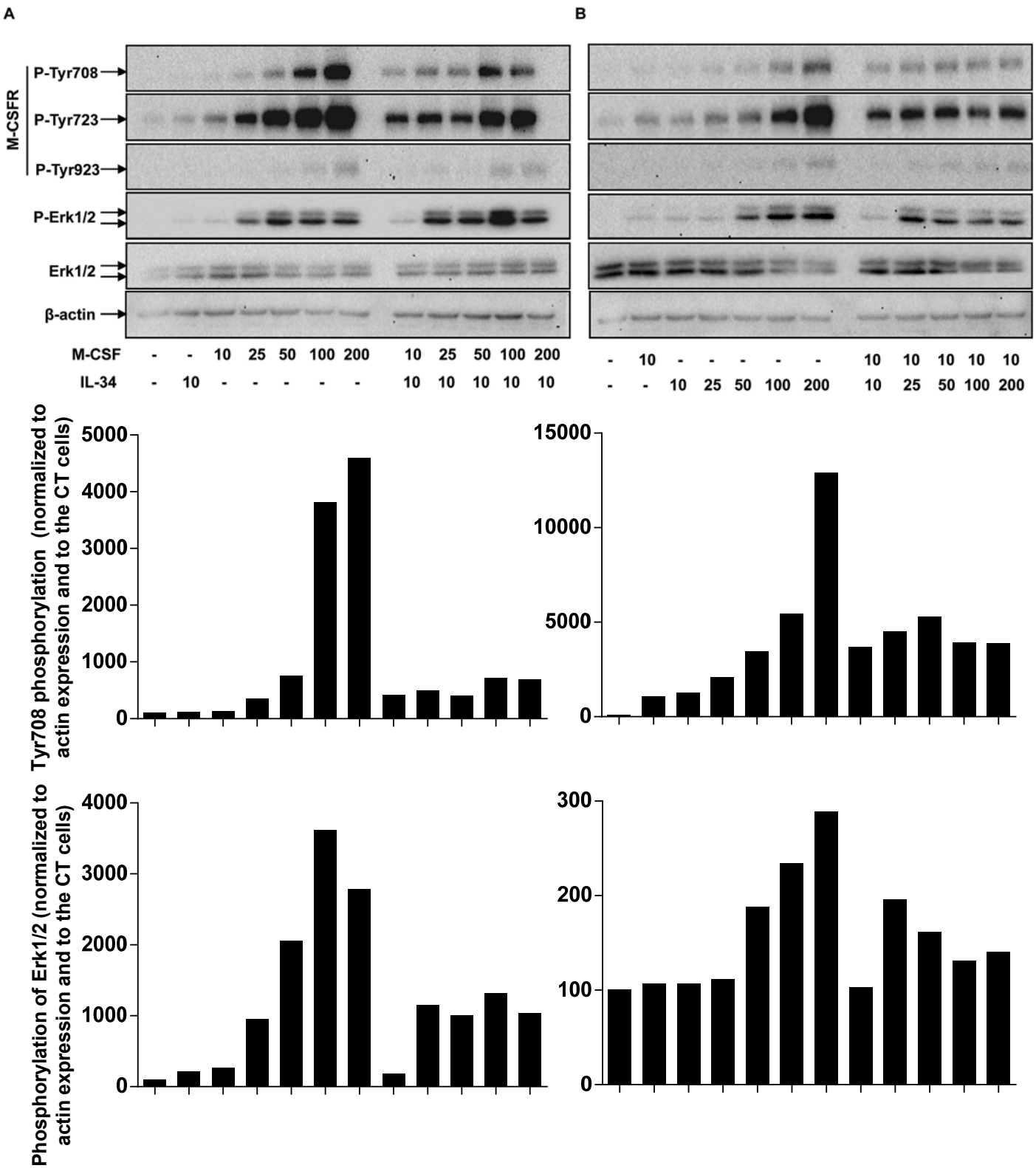

A
B
M-CSFR
P-Tyr708
P-Tyr723
P-Tyr923
P-Erk1/2
Erk1/2
β-actin
M-CSF - - 10 25 50 100 200 10 25 50 100 200
IL-34 - 10 - - - - - 10 10 10 10 10
- 10 - - - - - 10 10 10 10 10
- - 10 25 50 100 200 10 25 50 100 200
Tyr708 phosphorylation (normalized to actin expression and to the CT cells)
0 1000 2000 3000 4000 5000
0 5000 10000 15000
Phosphorylation of Erk1/2 (normalized to actin expression and to the CT cells)
0 1000 2000 3000 4000
0 100 200 300

Figure 2

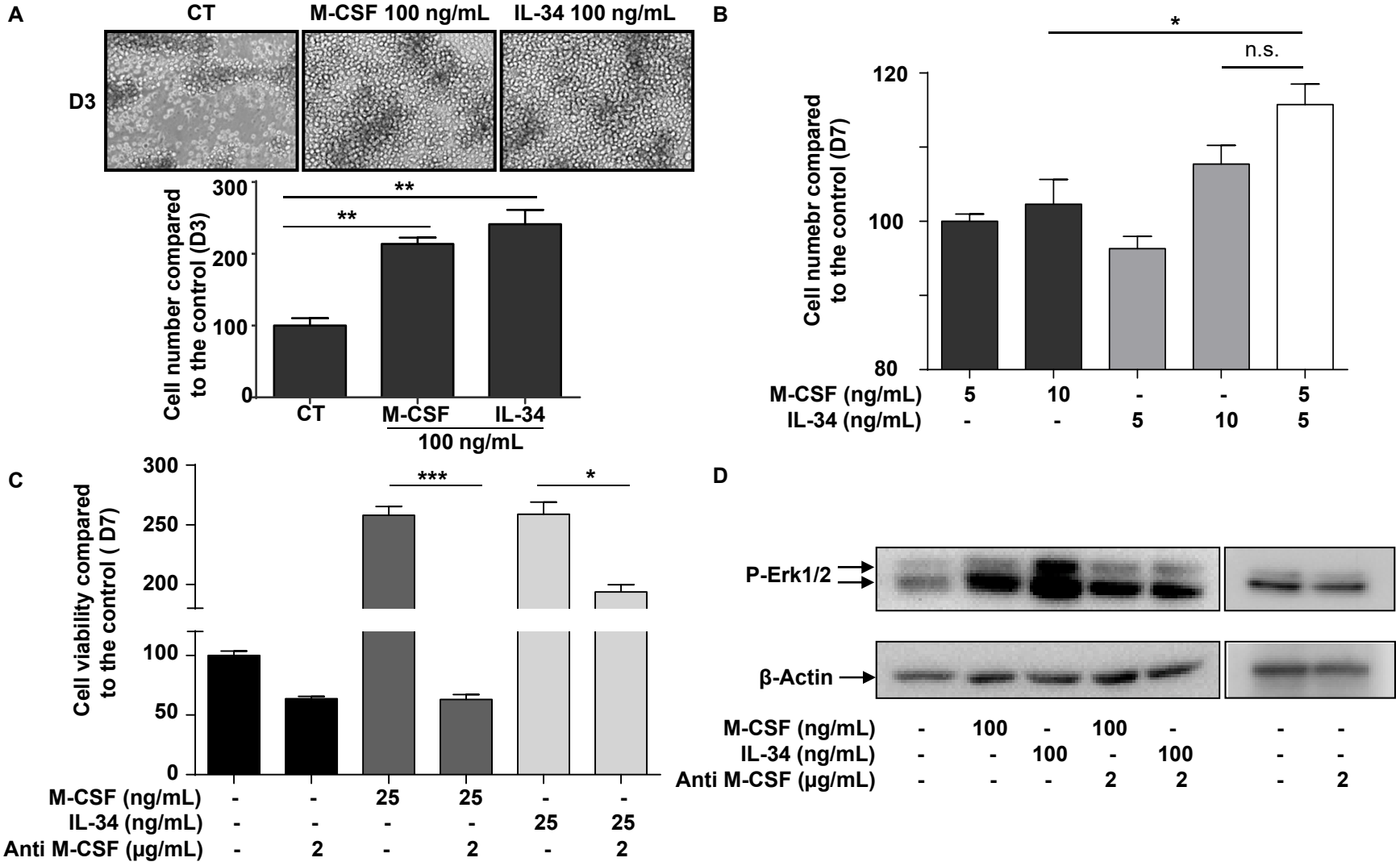

A
CT
M-CSF 100 ng/mL
IL-34 100 ng/mL
D3
Cell number compared to the control (D3)
300
200
100
0
**
**
CT
M-CSF
IL-34
100 ng/mL
B
*
n.s.
Cell numebr compared to the control (D7)
120
100
80
M-CSF (ng/mL) 5 10 - - 5
IL-34 (ng/mL) - - 5 10 5
C
Cell viability compared to the control (D7)
300
250
200
100
50
0
***
*
M-CSF (ng/mL) - - 25 25 - -
IL-34 (ng/mL) - - - - 25 25
Anti M-CSF (µg/mL) - 2 - 2 - 2
D
P-Erk1/2
β-Actin
M-CSF (ng/mL) - 100 - 100 - - -
IL-34 (ng/mL) - - 100 - 100 - -
Anti M-CSF (µg/mL) - - - 2 2 - 2

Figure 3

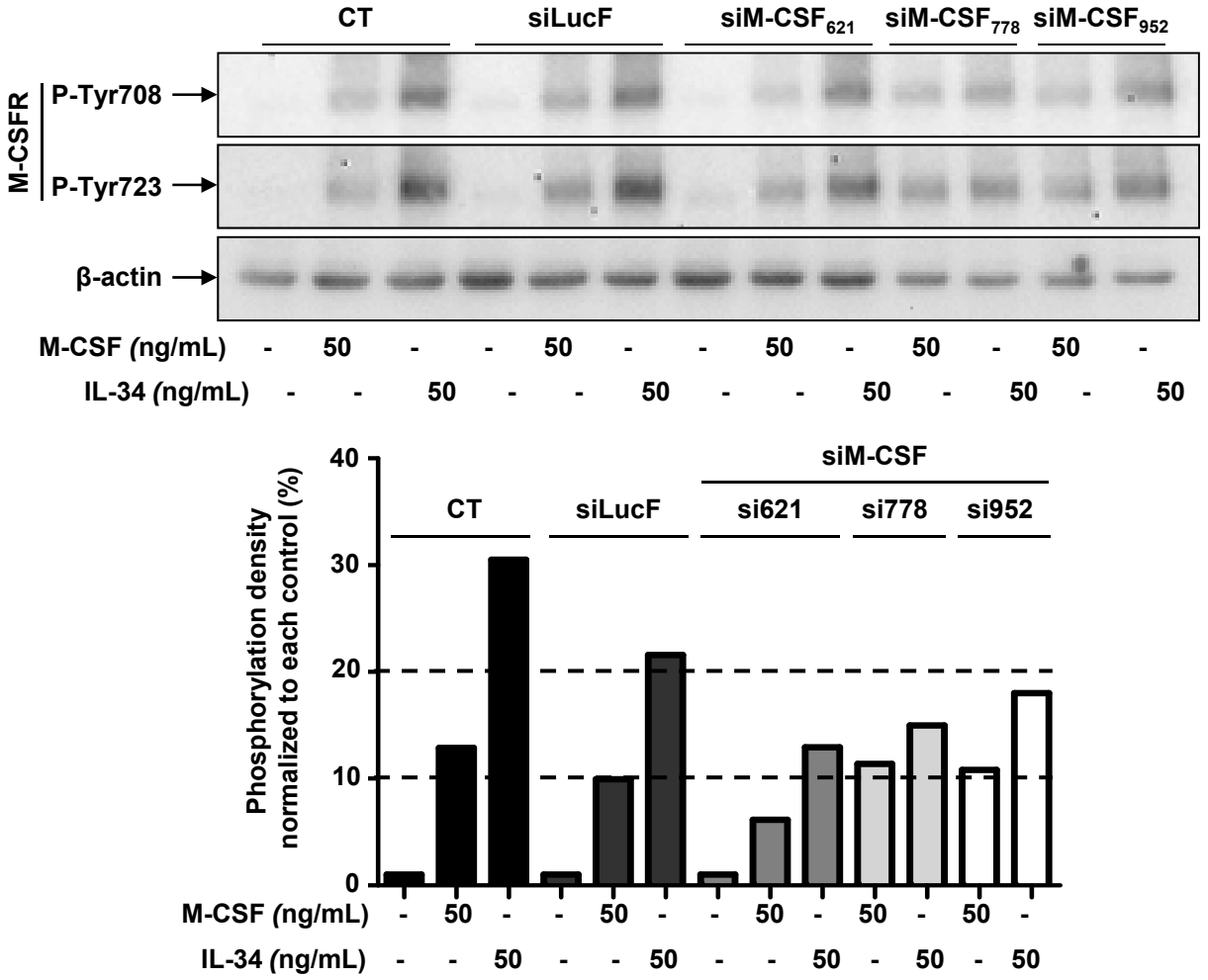

CT
siLucF
siM-CSF621
siM-CSF778
siM-CSF952
M-CSFR
P-Tyr708
P-Tyr723
β-actin
M-CSF (ng/mL) - 50 - - 50 - - 50 - 50 - 50 -
IL-34 (ng/mL) - - 50 - - 50 - - 50 - 50 - 50
siM-CSF
CT
siLucF
si621
si778
si952
Phosphorylation density normalized to each control (%)
40
30
20
10
0
M-CSF (ng/mL) - 50 - - 50 - - 50 - 50 - 50 -
IL-34 (ng/mL) - - 50 - - 50 - - 50 - 50 - 50

Figure 4

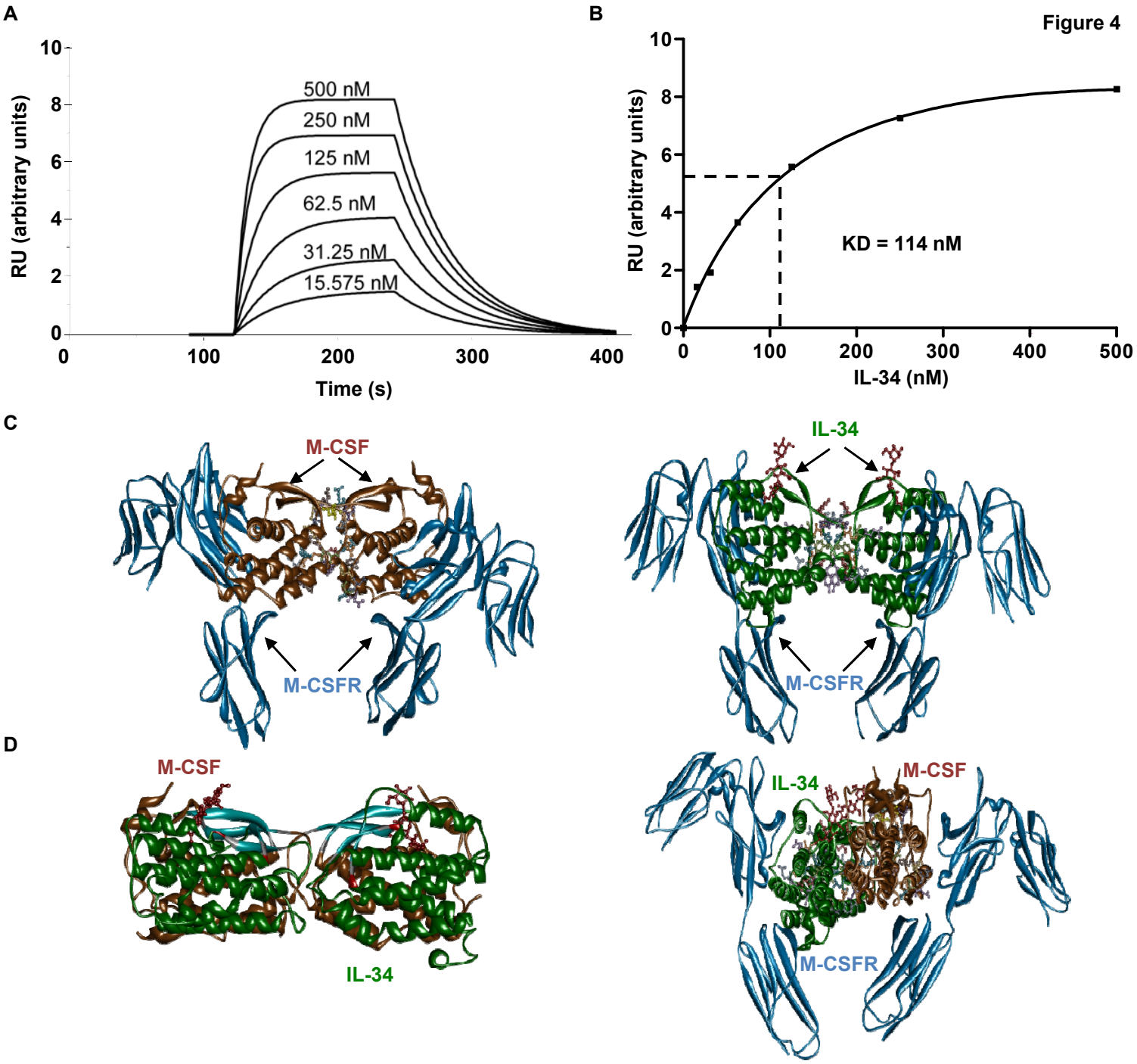

A
RU (arbitrary units)
Time (s)
500 nM
250 nM
125 nM
62.5 nM
31.25 nM
15.575 nM
B
RU (arbitrary units)
IL-34 (nM)
KD = 114 nM
C
M-CSF
M-CSFR
IL-34
M-CSFR
D
M-CSF
IL-34
IL-34
M-CSF
M-CSFR

Figure 5

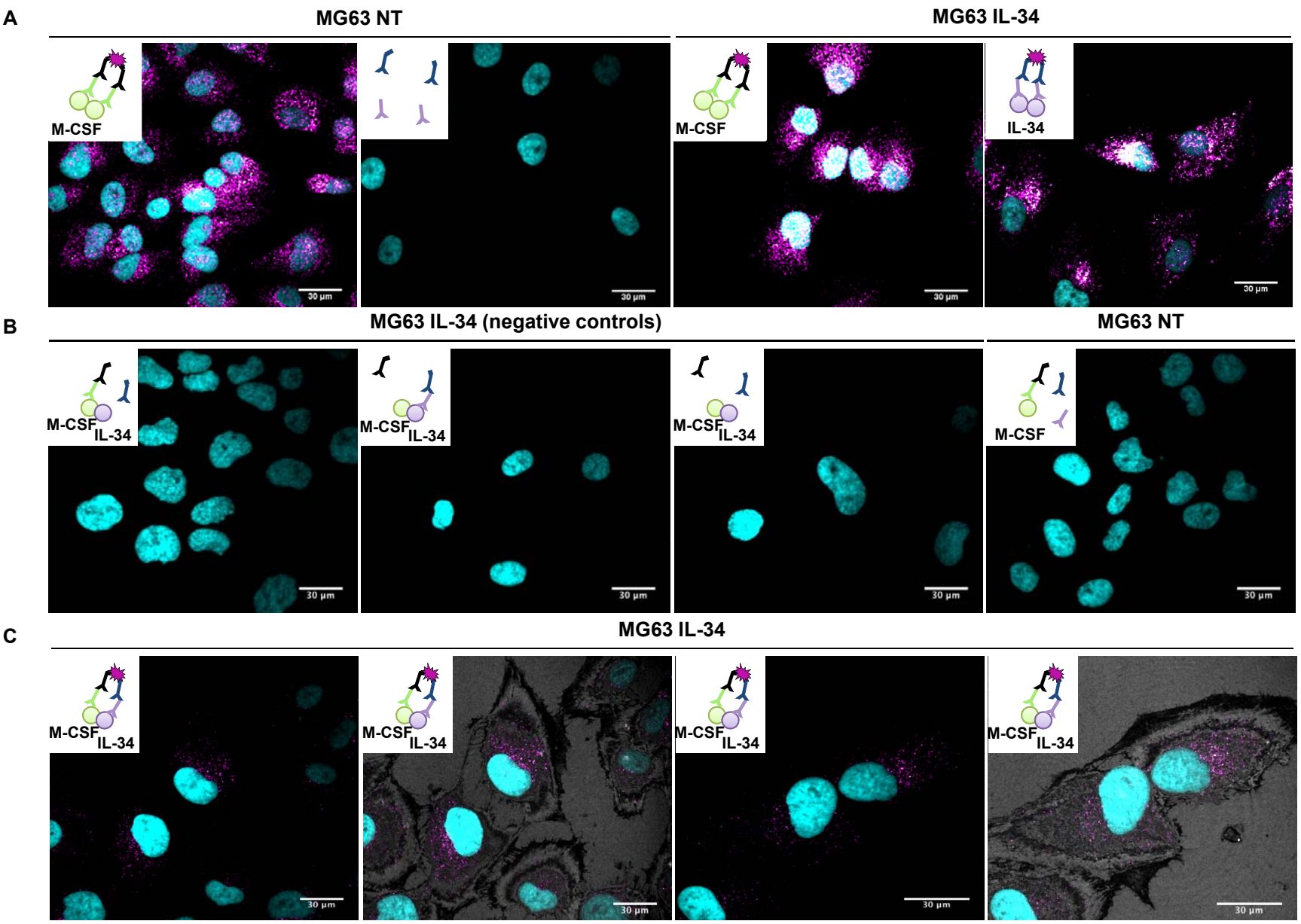

A
MG63 NT
MG63 IL-34
M-CSF
IL-34
30 µm
B
MG63 IL-34 (negative controls)
MG63 NT
M-CSF
IL-34
C
MG63 IL-34

Figure 6

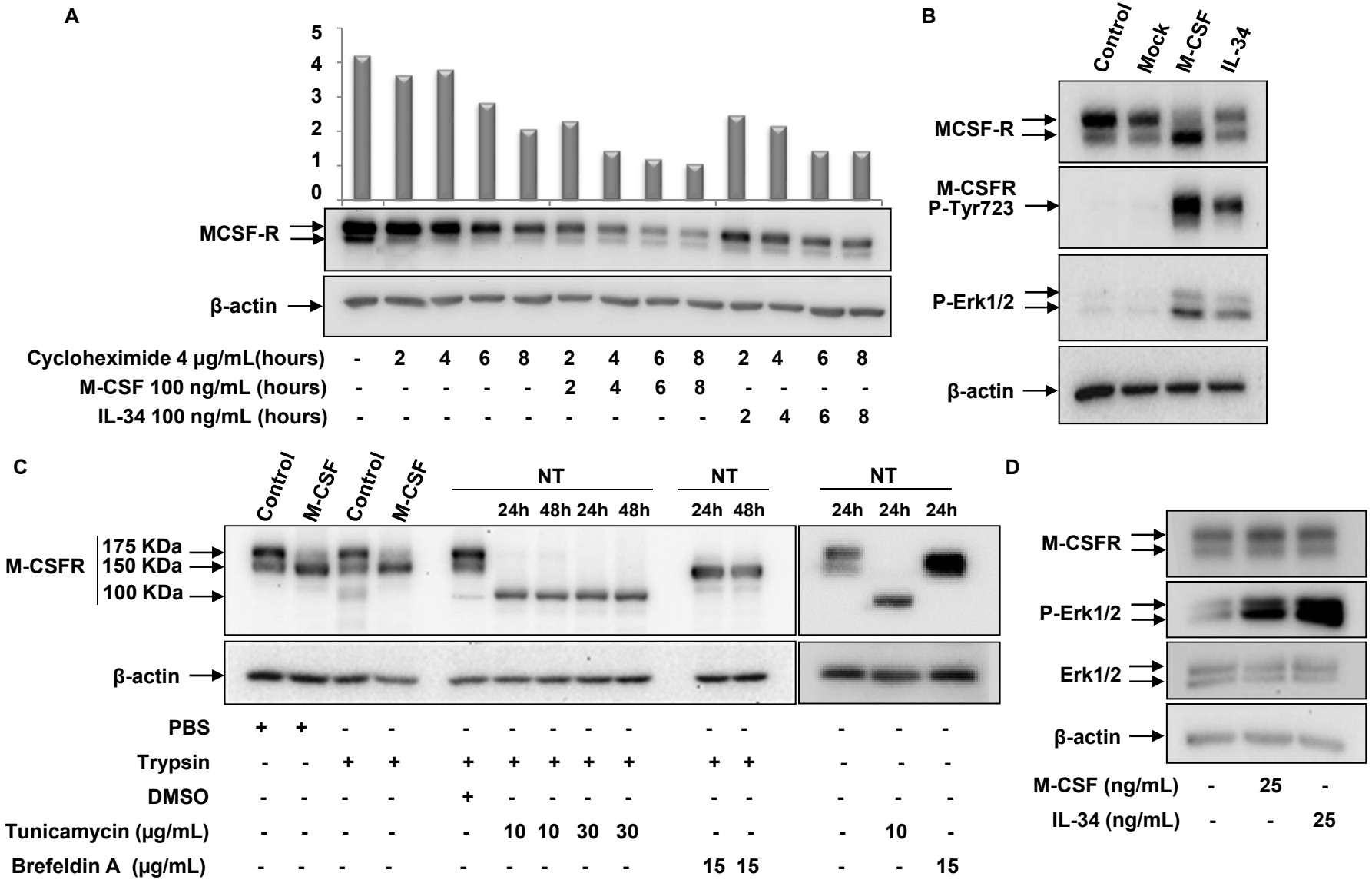

A
5
4
3
2
1
0
MCSF-R
β-actin
Cycloheximide 4 μg/mL(hours) - 2 4 6 8 2 4 6 8 2 4 6 8
M-CSF 100 ng/mL (hours) - - - - - 2 4 6 8 - - - -
IL-34 100 ng/mL (hours) - - - - - - - - - 2 4 6 8
B
Control
Mock
M-CSF
IL-34
MCSF-R
M-CSFR P-Tyr723
P-Erk1/2
β-actin
C
Control
M-CSF
Control
M-CSF
NT
24h 48h 24h 48h
NT
24h 48h
NT
24h 24h 24h
M-CSFR
175 KDa
150 KDa
100 KDa
β-actin
PBS + + - - - - - - - - - - - - -
Trypsin - - + + + + + + + + + - - -
DMSO - - - - + - - - - - - - - - -
Tunicamycin (μg/mL) - - - - - 10 10 30 30 - - - 10 -
Brefeldin A (μg/mL) - - - - - - - - - 15 15 - - 15
D
M-CSFR
P-Erk1/2
Erk1/2
β-actin
M-CSF (ng/mL) - 25 -
IL-34 (ng/mL) - - 25

Figure 7

